Received June 8, 2015, accepted July 8, 2015, date of publication July 28, 2015, date of current version August 7, 2015.

Digital Object Identifier 10.1109/ACCESS.2015.2461443

A Wideband Hybrid Water Antenna With an F-Shaped Monopole

LEI XING, YI HUANG, (Senior Member, IEEE), QIAN XU, AND SAQER ALJA'AFREH

Department of Electrical Engineering and Electronics, The University of Liverpool, Liverpool L69 3GJ, U.K.

Corresponding author: Y. Huang (Yi.Huang@liv.ac.uk)

ABSTRACT A new wideband hybrid antenna is proposed in this paper. It combines an F-shaped conducting monopole antenna and a water dielectric resonator antenna (DRA) to effectively broaden the antenna bandwidth. The F-shaped monopole is also used to excite the water DRA. The unique features of water, such as transparency and liquidity, allow complex feeding structures to be placed, and tuned inside the water DRA. A comprehensive parametric study is conducted to optimize the antenna performance. The final design is made and tested. A good agreement is obtained between the simulation and the measurement results. Compared with the conventional straight probe, the proposed antenna has a wider bandwidth from 410 to 870 MHz (a fractional bandwidth of 71.8%) for $S_{11} < -6$ dB, with a compact size (52 mm $\times$ 51.5 mm $\times$ 10 mm, roughly $0.071\lambda \times 0.07\lambda \times 0.0136\lambda$ at 410 MHz). It is shown that this new antenna is a very good candidate for hand-portable applications such as Digital Video Broadcasting–Handheld.

INDEX TERMS Hybrid antenna, water antenna, broadband antenna, dielectric resonator antenna, Digital Video Broadcasting–Handheld.

I. INTRODUCTION

Water antennas, a special case of liquid antennas, are a new type of antennas which have attracted increasing attentions in recent years [1]–[5]. By tuning the conductivity of water, water antennas can be considered as either DRAs or conducting antennas. They have attractive features such as: a) low-cost and readily accessible; b) compact size - water is a kind of high permittivity material. When it is used as a DRA, the antenna size can be reduced by a factor of $\sqrt{\varepsilon_r}$; c) conformability - it is easy to make the antenna to the desired shape; d) reconfigurability (physically, electrically and chemically) - the operational frequency and bandwidth may be controlled by the height and width of the liquid stream as well as the chemical composition; e) a small RCS (radar cross section) - it can be drained when not in use; f) easy to transport - especially for a large antenna and g) transparency. All these benefits open up new revenue for water antennas. In [1], a distilled water antenna with reconfigurable radiation patterns was proposed. Later, a broadband saline-water antenna was developed [2]. In [3], experimental investigation of the cylindrical water filled DRA was presented with a variable resonant frequency. In 2012, a monopole water antenna with a dielectric layer was reported, which has a very broad bandwidth [4]. A distilled water-based DRA was demonstrated with an application to measure the liquid real permittivity in [5]. In [6], water was used as the periodic grating to realize a reconfigurable radiation pattern.

In previous water antenna designs, the resonances of water itself have been used, resulting in either low efficiencies or narrow bandwidths. In the proposed design, the resonance of the feeding probe is utilized and it improves the radiation efficiency of the water antenna. By combining the resonances of the water DRA and the feeding probe, a wide bandwidth is realized. This hybrid technique has previously been employed in wideband DRAs [7]–[12], but here a new feeding structure is used for a liquid antenna, offering some new features and better performance.

The difficulties in using the resonance of the probe in a solid DRA are mainly in two aspects: 1) the probe length is limited by the DRA size; 2) the matching is sometimes difficult to achieve [13]. The liquidity and transparency of water allow a complex feeding structure (such as the F-shaped probe in this paper) to be implemented and easily tuned inside water, which would be difficult and expensive to realize in conventional solid dielectric materials such as ceramics.

In this paper, a wideband hybrid water antenna with an F-shaped probe feed is proposed to cover the frequency band from 470 to 862 MHz which is the typical frequency band for Digital Video Broadcasting–Handheld (DVB-H) [14]. To cover such a wide bandwidth while to maintain a very small size, the hybrid water antenna can be a promising solution. In comparison with other designs for this band, the main features of our design are in the following five aspects: 1) without using any active components and extra

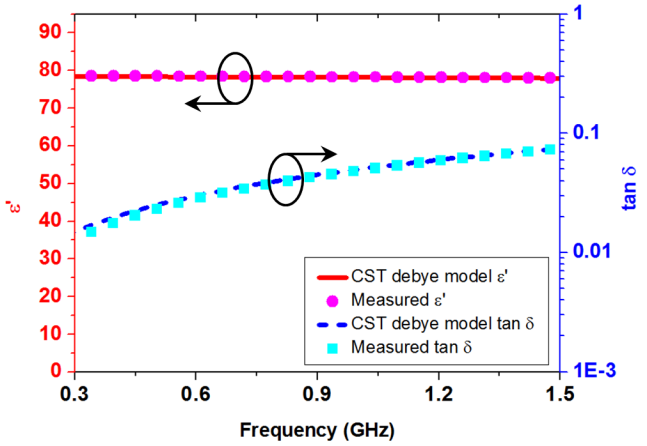

FIGURE 1. The real part of permittivity and loss tangent of the pure water at 25 °C from the measurement and CST Debye model.

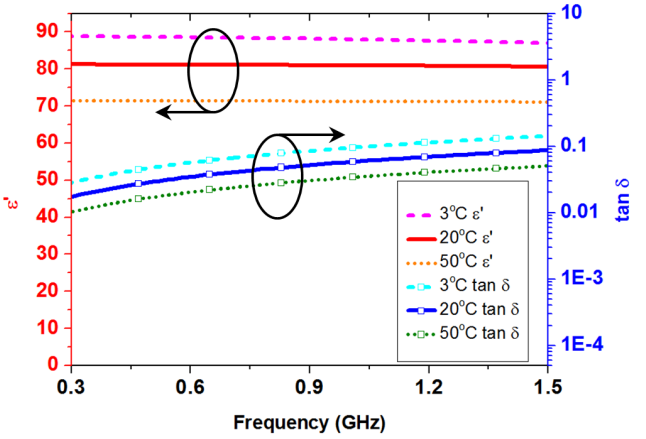

FIGURE 2. Measured real part of the permittivity and loss tangent of the pure water at different temperatures over the frequency of interest.

circuit, it achieves a fractional bandwidth of 71.8% with a low profile (10 mm); 2) the hybrid antenna structure combines an F-shaped monopole antenna and a metal coated DRA to produce a wideband response; 3) an efficient F-shaped probe feed is placed inside the water which would be difficult for conventional ceramic dielectric materials; 4) two sides of the water DRA are coated with metal patches to reduce the antenna size; 5) the antenna is optically transparent.

The paper is organized as follows: firstly, the water characteristics are evaluated and compared with the CST Debye model data and thermal characteristic of water is studied in Section II. Then, in sections III and IV, a new antenna is proposed and the physical insight behind the design is explored. Comprehensive parametric studies are performed and the effects of each part of the antenna are carefully examined in Section V. Finally, the water antenna with optimized parameters is fabricated. Experiments are conducted and the results are compared with simulation results in Section VI.

II. WATER CHARACTERISTICS FOR ANTENNA APPLICATION

Water is a kind of high permittivity material, the dielectric properties are a function of frequency and temperature [15]. Sometimes, water is not considered as a good dielectric as the loss increases with the frequency, especially at frequencies over 1 GHz. In this paper, we focus on the frequency band from 400 to 860 MHz. The loss is not significant, thus the water antenna can have a wide bandwidth and acceptable efficiency. The properties of pure water were measured using Agilent Dielectric Probe 85070 at room temperature (25°C) and the results are compared with CST Debye model as shown in Fig. 1, A very good agreement is obtained. The real part of the permittivity ε' is not sensitive to the frequency of interest. The temperature effects on its properties are also studied as shown in Fig. 2. By increasing the temperature of the pure water, the real part of the permittivity ε' and loss tangent $tan\delta$ decrease, which agrees with the conclusions in [16]. For cold climate areas, an antifreeze can be added to lower the freezing temperature point of the water.

III. ANTENNA CONFIGURATION

The geometry of the proposed antenna is shown in Fig. 3. It consists of a rectangular water layer with dimensions of $L_w \times W_w \times H_w$ (the dashed blue lines in Fig. 3 (d)), a holder with dimensions of $L_h \times W_h \times H_h$ and a ground plane with dimensions of $L_g \times W_g \times T_g$ ($230 \times 130 \times 1$ mm^3), corresponding to a standard DVB-H handheld receiver for a tablet PC or portable TV handset. The substrate (FR4) under the holder is used to support it. The material of the holder is set as acrylic plastic ($\varepsilon_r \approx 2.7 \sim 3$). The rectangular water layer and the holder can form a mixed DRA. An F-shaped feeding probe is inserted in the water layer horizontally to excite the antenna. The F-shaped feeding probe has three parts: the straight part has a length of L_p, the top folded part has a length of L_{pf}, the lower stub part has a length of L_s, a rotated angle of θ, and a location of Loc_s. Two metal patches (made of copper) are attached to the front and left side of the holder, respectively, reducing the resonant frequency of the DRA. Metal patch 1 in Fig. 3 (d) has dimensions of $L_{m1} \times (W_{m1} + T_h + H_w)$, where T_h is the thickness of the water holder. Metal patch 2 in Fig. 3 (c) has dimensions of $L_{m2} \times W_{m2}$. The holder has a displacement of D_h to the left edge of the ground plane.

IV. DESIGN OF RADIATION ELEMENT

In this section, the physical insights behind the design are discussed. The design procedures are summarized as follow:

1) By properly choosing the ratio ($H_h : H_w$) of the holder height to the water layer height, an effective permittivity around 20 to 30 can be obtained for the mixed DRA.

2) A metal coated DRA is designed to produce an upper band (i.e. around 850 MHz).

3) A dielectric loaded F-shaped monopole is designed to cover the lower and middle bands (i.e. from 440 to 600 MHz).

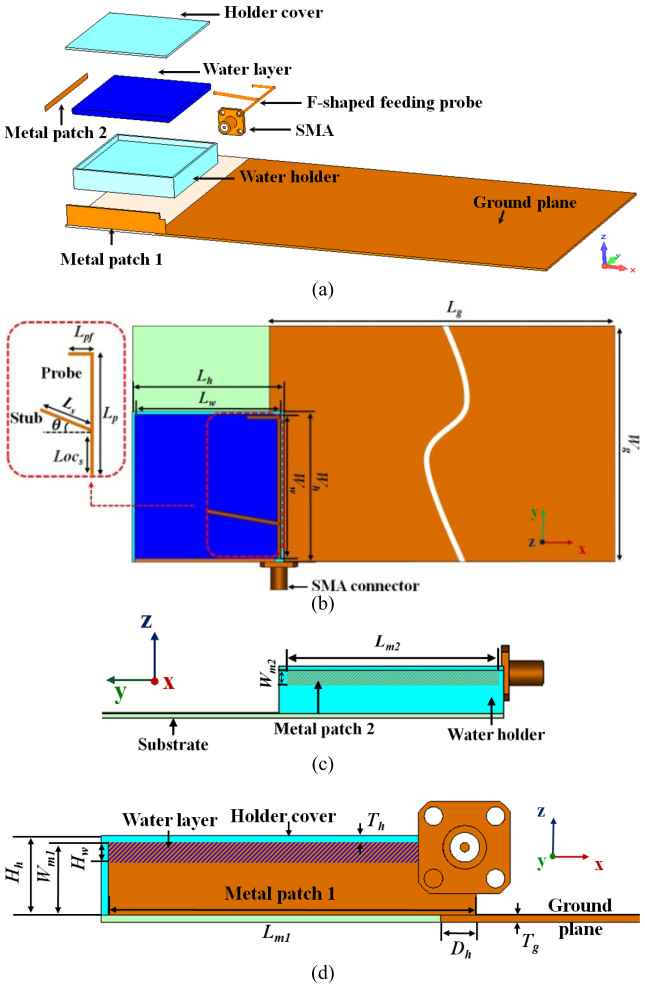

FIGURE 3. Geometry of the proposed antenna. (a) Exploded view. (b) Xoy plane view (holder cover is hidden). (c) Yoz plane view. (d) Xoz plane view.

A. DIELECTRIC MATERIAL CONSIDERATION

The high permittivity materials are usually considered for compact antenna designs. However, the bandwidth and Q factor have a trade-off. In this paper, the idea of effective relative permittivity is employed. By mixing a high permittivity material (water) with a low permittivity material (holder made of acrylic plastic), the combined effective relative permittivity is around 27 [17] with the water holder height and water height ratio $H_h : H_w = 70\% : 30\%$.

B. METAL COATED DRA MODE

For a specific material and frequency, various groups of DRA dimensions can be chosen. The strategy in this section is to fix one dimension a time, and plot the variations of the resonant frequency and Q factor as a function of the other two dimensions, and select a set of dimensions with the optimized size, desired frequency and Q factor.

To explain the process, an isolated rectangular DRA in Fig. 4 is used as an initial structure. By using a combination of magnetic wall model (MWM) and dielectric waveguide model (DWM) as stated in [18], the lowest mode $TE^z_{11\delta}$ mode and its dimensions can be estimated by following

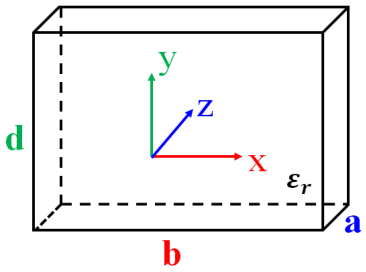

FIGURE 4. Isolated rectangular DRA.

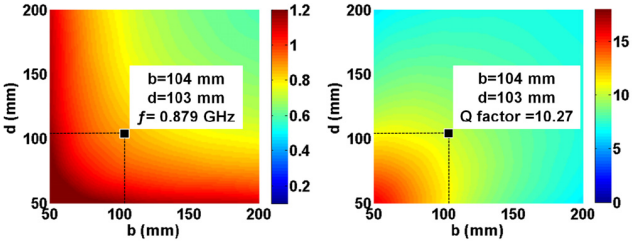

FIGURE 5. (a) The resonant frequency (as shown by the color in GHz) of TE^z_{111} mode as a function of dimensions *b* and *d*, (b) The Q factor (as shown by the color) of TE^z_{111} mode as a function of dimensions *b* and *d*.

equations [19]:

$$k_z \tan(k_z a/2) = \sqrt{(\varepsilon_r - 1)k_0^2 - k_z^2} \quad (1)$$

$$k_x^2 + k_y^2 + k_z^2 = \varepsilon_r k_0^2 \quad (2)$$

$$Q_{rad} = 2\omega_0 W_e / P_{rad} \quad (3)$$

where $k_x = \frac{\pi}{b}$, $k_y = \frac{\pi}{d}$, are the wavenumbers in x and y directions, respectively. k_0 denotes the free space wavenumber, z direction is the wave propagating direction. ω_0 represents the radian resonant frequency, W_e is the stored electric energy and P_{rad} stands for the radiated power. The calculated resonant frequency and Q factor for $TE^z_{11\delta}$ mode as functions of dimensions are shown in Fig. 5 (the values are presented in color).

Fig. 5 shows that the increase of the DRA dimensions will lead to the decrease of the resonant frequency and Q factor. From the plots, it is very convenient to choose the optimized dimensions with estimated resonant frequency and low Q factor. To integrate the DRA inside a hand portable device, we assume that one dimension is 10 mm, in this case, the optimized dimensions of the DRA are $a = 10$ mm, $b = 104$ mm, $d = 103$ mm, $f_{res} = 879$ MHz, Q factor $= 10.27$ as shown in Fig. 5. According to the E-field distribution of TE^z_{111} mode, two metal patches as shown in Fig. 3 are placed on two sides of the water DRA (to create electric-walls, alternatively a metallic paint or coating could be used), therefore the antenna size can be reduced to a quarter of the original one at the same frequency. After miniaturization, the final DRA dimensions are $a = 10$ mm, $b = 52$ mm, $d = 51.5$ mm ($f_{res} = 879$ MHz is a theoretically estimated frequency when the DRA is placed at the corner of the ground plane, the resonant frequency will be shifted downwards).

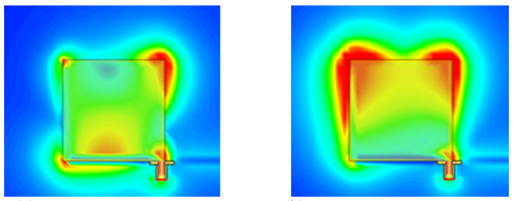

FIGURE 6. E-field distribution (magnitude) of the proposed antenna (without the stub). (a) 870 MHz, (b) 430 MHz.

Besides the dimensions and ε_r, this mode is also closely linked to the feeding probe. The feeding probe excites the DRA mode and also introduces a perfect electric conducting boundary which will change the field distribution inside the DRA. Without the probe, the desired mode of the DRA cannot be excited properly. The E-field distribution of the probe fed DRA is shown in Fig. 6 (a). It is noted that the E-field is mainly concentrated inside the DRA and a half cycle TE^z_{111} mode pattern is clearly observed.

C. F-SHAPED FEEDING PROBE MODE

To realize a wideband response, a dielectric (mixture of the water and holder) loaded F-shaped monopole is employed to cover the lower and middle bands (i.e. from 440 to 600 MHz), where the feeding probe simultaneously acts as a monopole antenna and the excitation of the DRA.

The lower band is mainly determined by the strong coupling between the feeding probe and metal patch 2. As can be seen in Fig. 6 (b), there is a current flow propagating from the feeding probe, then coupled to the metal patch 2 (on the left size), and radiated from both the feeding probe and metal patch, which is like a folded monopole antenna. The current forms a standing resonant wave with two peaks and one trough, the current path of this mode is around one wavelength at 430 MHz. The dielectric loading enhances the coupling considerably, also reduces the antenna size at this band. This coupling is well utilized to overcome the difficulties of achieving 430 MHz band by using compact size antennas.

To combine the upper and lower bands, a middle band associated with the stub is introduced. A comparison of S_{11} for the antenna with a conventional straight feeding probe and the proposed antenna is shown in Fig. 7. The proposed new design has a much wider bandwidth over the frequency of interest.

It should be mentioned that for whatever mode, the relevant radiator is the main radiator, and the other elements also make contributions to the improved characteristics of the proposed antenna.

V. PARAMETRIC STUDY

A number of parameters influence the performance of the hybrid water antenna, which include the water holder offset, the probe length, the stub length, the stub location, the stub rotate angle, and the ground plane dimensions. To investigate the effects of each part, parametric studies are performed. One parameter is changed at a time to observe its effects on the performance while other parameters are kept constant. The initial parameters are: $L_g = 230$ mm, $W_g = 130$ mm, $T_g = 1$ mm, $L_w = 50$ mm, $W_w = 49.5$ mm, $H_w = 2.7$ mm, $L_h = 52$ mm, $W_h = 51.5$ mm, $H_h = 10$ mm, $L_{m1} = 50$ mm, $W_{m1} = 10$ mm, $T_h = 1$ mm, $L_p = 50$ mm, $L_{pf} = 11$ mm, $L_s = 26$ mm, $\theta = 10°$, $Loc_s = 12$ mm, $D_h = 5$ mm.

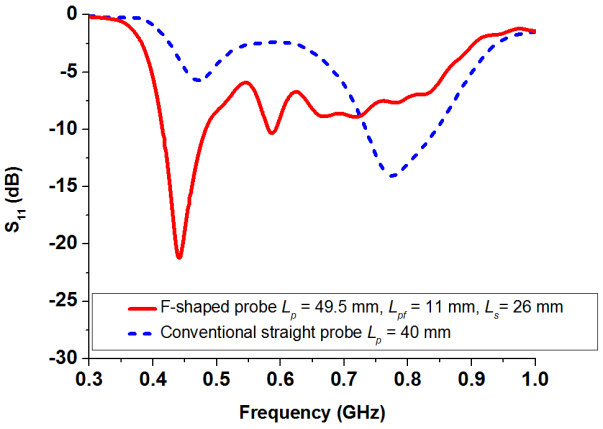

FIGURE 7. Simulated S_{11} comparison between the antenna with the conventional feeding probe and the proposed F-shaped feeding probe.

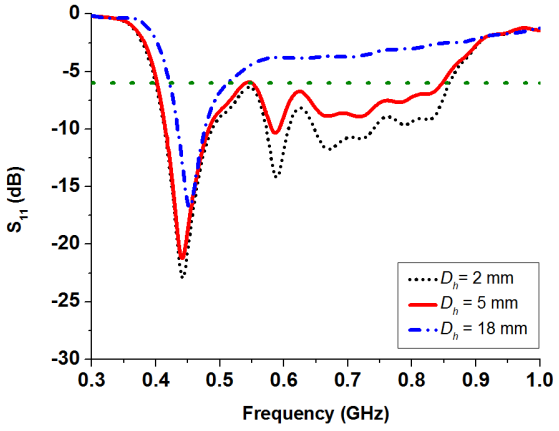

FIGURE 8. Simulated S_{11} with different values of D_h.

A. EFFECT OF THE WATER HOLDER OFFSET

To investigate the effects of the water holder offset, the simulated S_{11} (dB) with different values of D_h are plotted in Fig. 8. When the offset D_h is varied from 2 to 18 mm, the lower band around 440 MHz caused by the coupling between the F-shaped feeding probe and metal patch 2 as shown in Fig. 6(b) is quite stable while the impedance matching at higher frequencies becomes worse. This is because the matching at higher frequencies (around 800 MHz) is mainly determined by the metal coated DRA. By increasing the value of D_h, the space dielectric resonator (DR) covered by the ground plane increases which changes the boundary conditions. Decreasing the value of D_h leads to a wider bandwidth response which also increases the difficulty in fabrication. A trade-off between the achievable bandwidth and practical fabrication has been considered by choosing $D_h = 5$ mm in the final design.

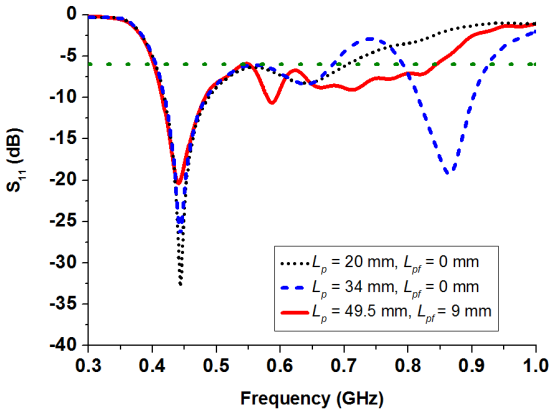

FIGURE 9. Simulated S_{11} with different values of L_p and L_{pf}.

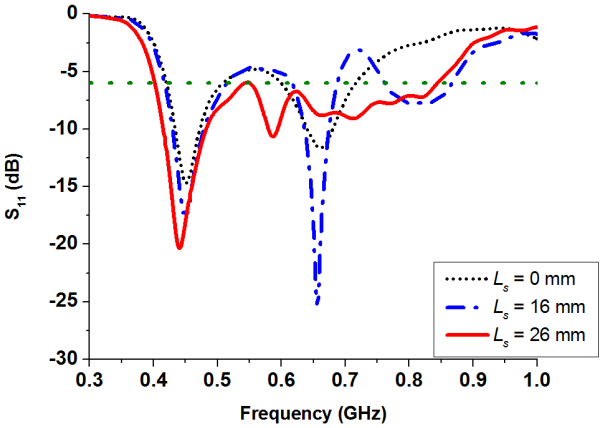

FIGURE 10. Simulated S_{11} with different values of L_s.

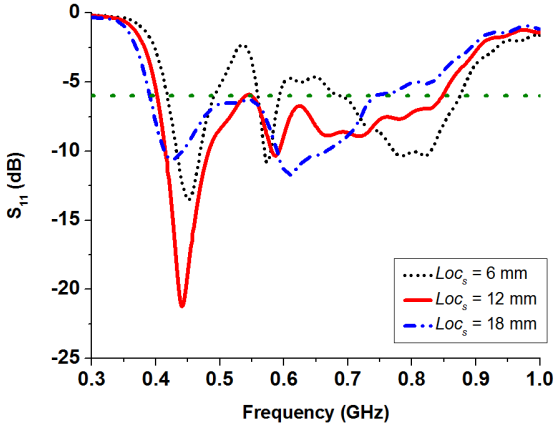

FIGURE 11. Simulated S_{11} with different values of Loc_s.

B. EFFECT OF THE PROBE LENGTH

As a hybrid antenna, the feeding probe has two functions, namely excitation and radiation. To investigate the effects of the probe length, the simulated S_{11} as a function of L_p and L_{pf} is shown in Fig. 9. When the probe is short, the metal coated DRA is not properly excited, only two frequency bands are observed (black dotted line in Fig. 9), one is mainly caused by the coupling between the feeding probe and metal patch 2 (as the stub is quite long, the coupling is not greatly affected by the probe length), the other is from the stub. As the probe length increases, the metal coated DRA is excited; three separate bands appear (blue dash line in Fig. 9). By further increasing the probe length, the upper band determined by the metal coated DRA shifts downwards. Thus three bands are combined and a wide bandwidth can be achieved when $L_p = 49.5$, $L_{pf} = 11$ mm (red solid line in Fig. 9).

C. EFFECT OF THE STUB LENGTH, LOCATION AND ROTATE ANGLE

As water is a liquid dielectric material, a stub can be placed inside the water as shown in Fig. 3(b) to tune the impedance matching and also introduce a frequency band. Such a matching circuit is convenient, since no lumped elements are required. To better understand the importance of the stub in achieving a wideband response, the effects of the stub length, location and rotate angle are investigated.

As shown in Fig. 10, when $L_s = 0$ mm, the antenna covers two separate bands, 400 to 500 MHz band and 620 to 720 MHz band for $S_{11} < -6$ dB, corresponding to two troughs in black dot line in Fig. 10. These two bands are associated with coupling between the F-shaped probe and metal patch 2, and the metal coated DRA, respectively. By soldering the stub to the feeding probe, a third frequency band in blue dash dot line from 780 to 880 MHz is introduced. As L_s increases, the third frequency band shifts downwards and becomes the middle band. Meanwhile, the frequency band associated with the metal coated DRA shifts upwards, since the field inside the water DRA is disturbed by the changing of the stub length. By combining these three different bands, a maximum -6 dB bandwidth can be achieved when $L_s = 26$ mm.

Besides the stub length, the stub location is also an important parameter affecting the performance of the antenna. By changing the location of the stub, the field inside the DRA is altered, which affects the impedance matching of the frequency band from 700 to 850 MHz. It is observed in Fig. 11, as the Loc_s is increased, the lower band caused by the coupling is quite stable; while the frequency band associated the stub and the water DRA is affected. If Loc_s is further increased, it could lead the bands associated with the stub and the water DRA over-merged at $Loc_s = 18$ mm corresponding to the blue dash dot line in Fig. 11. Separating these three bands properly leads to a larger bandwidth.

Due to the transparency and liquidity of water, the stub can be easily tuned inside the water which provides a degree of control on the impedance matching over a wide band. It is noted in Fig. 12, by decreasing θ from 30° to 10°, it mainly affects the middle and higher bands, as the field inside the water will be disturbed and the bands introduced by the stub will be affected. For a smaller value of θ such as $\theta = -20°$, the lower band will also be affected, because the coupling between the F-shaped probe and metal patch 2 will be weaker when θ is negative. At $\theta = 10°$, the maximum -6 dB bandwidth can be obtained.

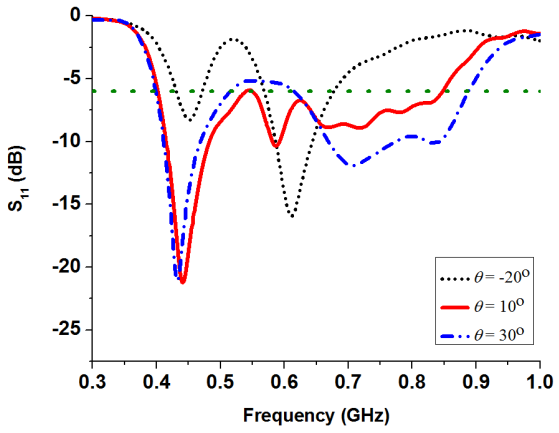

FIGURE 12. Simulated S_{11} with different values of θ.

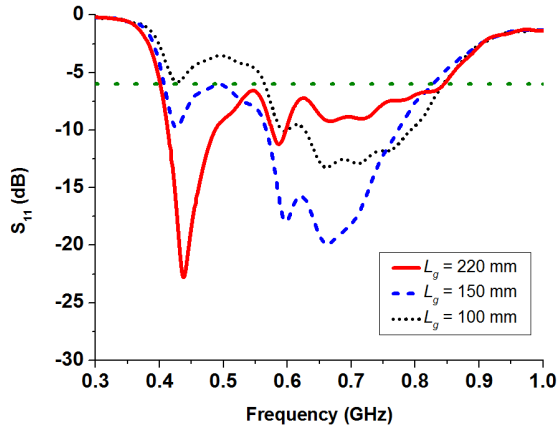

FIGURE 13. Simulated S_{11} with different values of L_g.

D. EFFECT OF THE GROUND PLANE SIZE

The variations of S_{11} (dB) for different values of L_g have been compared to explore the ground plane effects. Usually, for hand-portable applications such as mobile phones, the ground plane will be part of the radiating element, influencing the input impedance of the antenna. It is observed in Fig. 13, for a given ground plane width $W_g = 130$ mm, the ground plane length affects the impedance matching of the antenna, but its effect on the lower band is bigger. When L_g is decreased from 220 to 100 mm, the impedance matching of the lower band is getting worse (the real part of impedance at 430MHz is increased from 50 to 82 ohm), however, the -6 dB bandwidth across the whole band is stable, which is good for some space limited applications such as mobile phones, the ground plane can be reduced to save more space for other components. When the L_g is further reduced to 100 mm, the impedance matching of the lower band will become worse (the real part of impedance at 430 MHz is 128 ohm), and the lower band gradually separate with other bands. It is necessary to place the metal coated DRA on a ground plane with $L_g \times W_g = 150$ mm $\times$ 130 mm to promise a wideband performance. The ground plane size affects the impedance matching as well as the total efficiency of the antenna. A higher total efficiency can be obtained when the antenna is well matched.

The effects of various parameters on the antenna performance have now been carefully examined. Some interesting conclusions can be summarized as follows:

1) The selection of the water holder offset is very important in achieving the broad bandwidth, as it will affect the impedance matching at higher frequencies. Decreasing the value of D_h leads to a wider bandwidth response but also increases the difficulty in fabrication. A trade-off has to be considered between the achievable bandwidth and practical fabrication.

2) The probe length is also a critical parameter. The DRA mode cannot be properly excited, if the probe is too short. By increasing the length of the probe, the upper band shifts downwards.

3) The stub introduces a new band and also affects the impedance matching, as it will affect the field distribution inside the DRA. At a certain stub length, location and angle, the bandwidth can be maximized.

4) The ground plane size will influence the impedance matching and total efficiency of the antenna. The effects on the lower band are bigger, as the real part of the impedance at the lower band will be affected by the variations of ground plane size. In order to obtain a wide bandwidth, it is necessary to place the metal coated DRA on a ground plane with $L_g \times W_g = 150 \times 130$ mm^2.

5) As shown in Fig. 6(b), a resonant mode is generated near 430 MHz, thus in all results we can see a trough in S_{11} near this frequency.

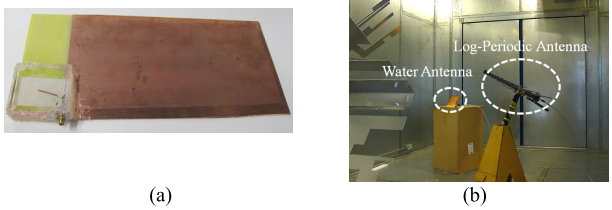

(a) (b)

FIGURE 14. (a) Prototype of the water antenna, (b) RC set-up for antenna efficiency test.

VI. EXPERIMENTAL MEASUREMENTS AND RESULTS

To verify the design, an F-shaped probe feed hybrid water antenna was fabricated; the prototype of the proposed antenna is shown in Fig. 14 (a). The optimal parameters are $L_g = 230$ mm, $W_g = 130$ mm, $T_g = 1$ mm, $L_w = 50$ mm, $W_w = 49.5$ mm, $H_w = 2.7$ mm, $L_h = 52$ mm, $W_h = 51.5$ mm, $H_h = 10$ mm, $L_{m1} = 50$ mm, $W_{m1} = 10$ mm, $T_h = 1$ mm, $L_p = 49.5$ mm, $L_{pf} = 11$ mm, $L_s = 26$ mm, $\theta = 10°$, $Loc_s = 12$ mm, $D_h = 5$ mm. The S_{11}, radiation pattern, and realized gain were measured in an anechoic chamber. And the radiation efficiency (defined as the ratio of the power radiated to the power accepted by the antenna port) was measured in a reverberation chamber (RC)

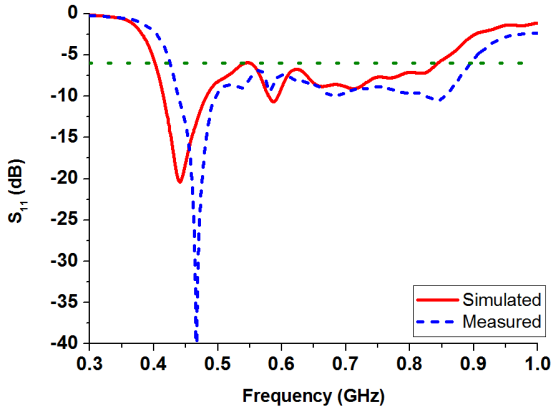

FIGURE 15. Measured and simulated S_{11} (dB) of the proposed antenna.

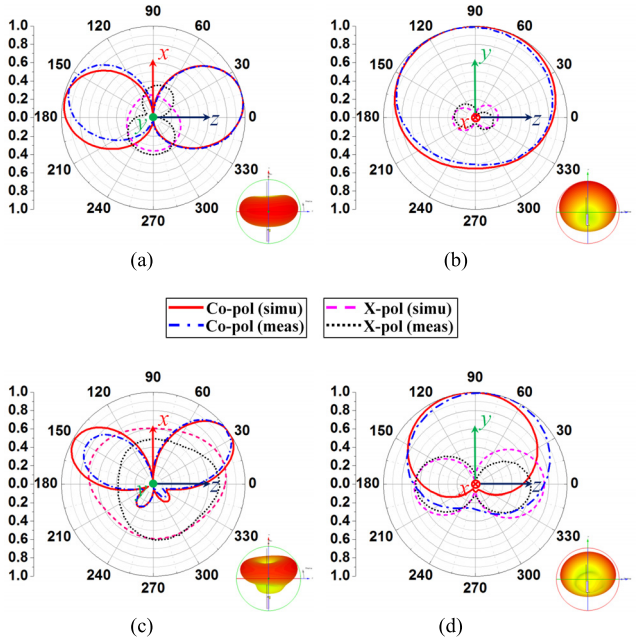

FIGURE 16. 2-D radiation patterns of the proposed antenna at (a) f = 460MHz, xoz plane, (b) f = 460MHz, yoz plane, (c) f = 700MHz, xoz plane, (d) f = 700MHz, yoz plane.

by using the two-antenna approach described in [20]. The RC setup for the antenna efficiency test is shown in Fig. 14 (b).

The simulated and measured results are compared in terms of S_{11}, radiation pattern, realized gain as well as radiation efficiency as shown in Figs 15 - 18. It is evident that the hybrid water antenna has a very broadband from 410 to 870 MHz for $S_{11} < -6$ dB (the fractional bandwidth > 70%). The radiation patterns corresponding to the polarization of antenna are plotted at 460 and 700 MHz, respectively. In the radiation pattern measurement, the E-field parallel to the antenna rotation plane is defined as the co-polarization (co-pol). In order to avoid the cable effects, an RF choke was used in the measurement. The realized gain was measured in the direction of $\theta = 90°$, $\varphi = 45°$, again a good agreement is observed. As a reference, the maximum gain (a function of frequency) is added. The discrepancies between

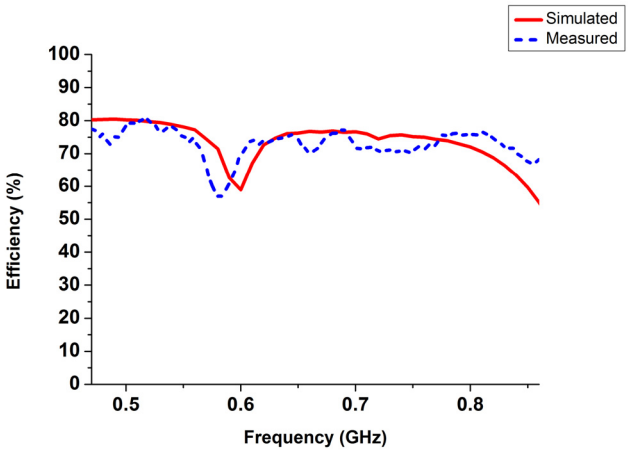

FIGURE 17. Measured and simulated radiation efficiency of the proposed antenna.

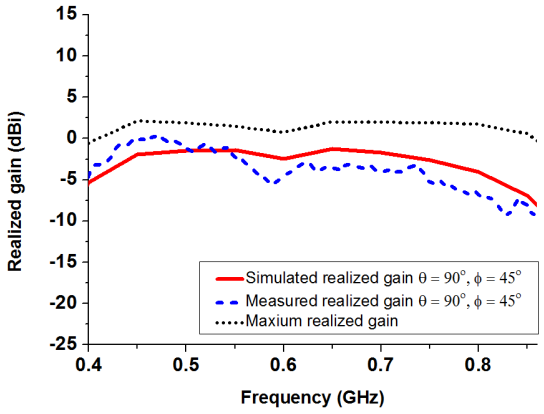

FIGURE 18. Measured and simulated realized gain at the direction of $\theta = 90°$, $\varphi = 45°$ of the proposed antenna.

the simulations and measurements are mainly caused by two reasons: 1) fabrication error; 2) the material difference. The radiation efficiency of the antenna is larger than 70% across the whole frequency band, except for the band around 600MHz. The E-field has a strong distribution in the water at the band around 600 MHz, causing more power loss ($\frac{1}{2}\int_V \vec{J}\cdot\vec{E}^* dV = \frac{\omega\varepsilon''}{2}\int_V |\vec{E}|^2 dV$), thus induces the dip in the radiation efficiency plot. Overall, a good agreement is achieved.

VII. CONCLUSIONS

A low profile, wideband hybrid water antenna has been proposed. An F-shaped conducting probe placed inside the water has been designed to efficiently excite the water DRA and also work as a radiating element. Two metal patches have been added to specific faces of the structure to reduce the antenna size. The coupling between the feeding probe and the metal patch is well utilized to cover a lower band around 430 MHz, which is very hard to achieve for compact antennas. Three different bands associated with the strong coupling between the feeding probe and metal patches; the stub and the metal coated DRA have been effectively combined to realize a wideband response. The antenna has

used the unique features of water in terms of the high permittivity, transparency and convenience/flexibility to incorporate the complex feeding structures inside the water DRA. A comprehensive parametric study has been performed and the effects of various parameters on the antenna performance have been carefully examined. Measurements have been conducted and the results agree well with the simulations. It has been demonstrated that by using the F-shaped feeding probe, this hybrid antenna covers a very wide bandwidth from 410 to 870 MHz (a fractional bandwidth of 71.8%) with a compact size ($52 \times 51.5 \times 10$ mm^3, roughly $0.071\lambda \times 0.07\lambda \times 0.0136\lambda$ at 410 MHz) and high radiation efficiency (over 60%).

This work has successfully demonstrated the attractive features of water-based antenna. The results show that the hybrid structure with combination of the conducting antenna and DRA is potentially very useful for low frequency, wideband applications. The research is extremely valuable for the water antenna development. The proposed water antenna can be a very promising candidate for hand-portable applications such as DVB-H.

It should be pointed out that there is a concern on the temperature-dependent performance of water-based antennas. This can be addressed by adding special materials (such as antifreeze), also the applications we are interested are mainly for domestic room temperature. For some extreme cases, this design may not be directly applicable, but the idea of the design is still valid.

REFERENCES

[1] S. P. Kingsley and S. G. O'Keefe, "Beam steering and monopulse processing of probe-fed dielectric resonator antennas," *IEE Proc.-Radar, Sonar Navigat.*, vol. 146, no. 3, pp. 121–125, Jun. 1999.
[2] H. Fayad and P. Record, "Broadband liquid antenna," *Electron. Lett.*, vol. 42, no. 3, pp. 133–134, Feb. 2006.
[3] S. G. O'Keefe and S. P. Kingsley, "Tunability of liquid dielectric resonator antennas," *IEEE Antennas Wireless Propag. Lett.*, vol. 6, pp. 533–536, Nov. 2007.
[4] L. Xing, Y. Huang, S. S. Alja'afreh, and S. J. Boyes, "A monopole water antenna," in *Proc. Loughborough Antennas Propag. Conf. (LAPC)*, Loughborough, U.K., Nov. 2012, pp. 1–4.
[5] R. Zhou, H. Zhang, and H. Xin, "Liquid-based dielectric resonator antenna and its application for measuring liquid real permittivities," *IET Microw., Antennas Propag.*, vol. 8, no. 4, pp. 255–262, Mar. 2014.
[6] Z. Hu, Z. Shen, and W. Wu, "Reconfigurable leaky-wave antenna based on periodic water grating," *IEEE Antennas Wireless Propag. Lett.*, vol. 13, pp. 134–137, Jan. 2014.
[7] M. Lapierre, Y. M. M. Antar, A. Ittipiboon, and A. Petosa, "Ultra wideband monopole/dielectric resonator antenna," *IEEE Microw. Wireless Compon. Lett.*, vol. 15, no. 1, pp. 7–9, Jan. 2005.
[8] K. Lan, S. K. Chaudhuri, and S. Safavi-Naeini, "Design and analysis of a combination antenna with rectangular dielectric resonator and inverted L-plate," *IEEE Trans. Antennas Propag.*, vol. 53, no. 1, pp. 495–501, Jan. 2005.
[9] Y. Gao, B.-L. Ooi, W.-B. Ewe, and A. P. Popov, "A compact wideband hybrid dielectric resonator antenna," *IEEE Microw. Wireless Compon. Lett.*, vol. 16, no. 4, pp. 227–229, Apr. 2006.
[10] T.-H. Chang and J.-F. Kiang, "Broadband dielectric resonator antenna with metal coating," *IEEE Trans. Antennas Propag.*, vol. 55, no. 5, pp. 1254–1259, May 2007.
[11] L. Huitema, M. Koubeissi, M. Mouhamadou, E. Arnaud, C. Decroze, and T. Monediere, "Compact and multiband dielectric resonator antenna with pattern diversity for multistandard mobile handheld devices," *IEEE Trans. Antennas Propag.*, vol. 59, no. 11, pp. 4201–4208, Nov. 2011.
[12] Y. M. Pan, S. Y. Zheng, and W. Li, "Dual-band and dual-sense omnidirectional circularly polarized antenna," *IEEE Antennas Wireless Propag. Lett.*, vol. 13, pp. 706–709, Apr. 2014.
[13] A. Buerkle, K. Sarabandi, and H. Mosallaei, "Compact slot and dielectric resonator antenna with dual-resonance, broadband characteristics," *IEEE Trans. Antennas Propag.*, vol. 53, no. 3, pp. 1020–1027, Mar. 2005.
[14] *Digital Video Broadcasting (DVB); DVB-H Implementation Guidelines*, ETSI Standard TR 102 377 V1.4.1 (2009-06), 2009.
[15] W. Ellison *et al.*, "New permittivity measurements of seawater," *Radio Sci.*, vol. 33, no. 3, pp. 639–648, May/Jun. 1998.
[16] W. J. Ellison, "Permittivity of pure water, at standard atmospheric pressure, over the frequency range 0-25 THz and the temperature range 0-100 °C," *J. Phys. Chem. Ref. Data*, vol. 36, no. 1, pp. 1–18, 2007.
[17] T. Nakamura, M. Shimizu, H. Kimura, and R. Sato, "Effective permittivity of amorphous mixed materials," *Electron. Commun. Jpn. I, Commun.*, vol. 88, no. 10, pp. 1–9, Oct. 2005.
[18] E. A. J. Marcatili, "Dielectric rectangular waveguide and directional coupler for integrated optics," *Bell Syst. Technol. J.*, vol. 48, no. 7, pp. 2071–2102, Sep. 1969.
[19] R. Kumar Mongia and A. Ittipiboon, "Theoretical and experimental investigations on rectangular dielectric resonator antennas," *IEEE Trans. Antennas Propag.*, vol. 45, no. 9, pp. 1348–1356, Sep. 1997.
[20] C. L. Holloway, H. A. Shah, R. J. Pirkl, W. F. Young, D. A. Hill, and J. Ladbury, "Reverberation chamber techniques for determining the radiation and total efficiency of antennas," *IEEE Trans. Antennas Propag.*, vol. 60, no. 4, pp. 1758–1770, Apr. 2012.

LEI XING received the B.Eng. and M.Eng. degrees from the School of Electronics and Information, Northwestern Polytechnical University, Xi'an, China, in 2009 and 2012, respectively. She is currently pursuing the Ph.D. degree in electrical engineering with The University of Liverpool, U.K.

Her current research interests include water antennas, hand-portable antennas, and reconfigurable antennas. She received the Best Student Award at the Fifth U.K./Europe–China Workshop on Millimeter Waves and Terahertz Technologies in 2012.

YI HUANG (S'91–M'96–SM'06) received the B.Sc. degree in physics from Wuhan University, China, the M.Sc. (Eng.) degree in microwave engineering from NRIET, Nanjing, China, and the D.Phil. degree in communications from the University of Oxford, Oxford, U.K., in 1994.

He was a Research Fellow with British Telecom Laboratories in 1994, and then joined the Department of Electrical Engineering and Electronics, The University of Liverpool, U.K., as a Faculty Member, in 1995, where he is currently a Full Professor of Wireless Engineering, the Head of the High Frequency Engineering Research Group, and the M.Sc. Program Director. He has been conducting research in the areas of wireless communications, applied electromagnetics, radar, and antennas for the past 25 years. His experience includes three years with NRIET as a Radar Engineer and various periods with the University of Birmingham, the University of Oxford, and the University of Essex, U.K., as a Research Staff Member. He has authored over 200 refereed papers in leading international journals and conference proceedings, and is the principal author of the popular book entitled *Antennas: From Theory to Practice* (Wiley, 2008). He has received many research grants from research councils, government agencies, charity, EU, and industry, acted as a Consultant to various companies, and served on a number of national and international technical committees.

Prof. Huang has been an Editor, an Associate Editor, or a Guest Editor of four international journals. He has been a Keynote/Invited Speaker and Organizer of many conferences and workshops (e.g., the IEEE iWAT 2010, WiCom 2006 and 2010, and LAPC 2012). He is the Editor-in-Chief of *Wireless Engineering and Technology*, a U.K. National Representative of European COST-IC1102, an Executive Committee Member of the Institution of Engineering and Technology (IET) Electromagnetics Professional Network, and a fellow of IET in U.K.

QIAN XU received the B.Eng. and M.Eng. degrees from the School of Electronics and Information, Northwestern Polytechnical University, Xi'an, China, in 2007 and 2010, respectively. He is currently pursuing the Ph.D. degree in electrical engineering with The University of Liverpool, U.K.

He was an RF Engineer in Nanjing, China, in 2011, and an Application Engineer with CST, Shanghai, China, in 2012. His current research interests include computational electromagnetics, reverberation chamber, and anechoic chamber.

SAQER ALJA'AFREH received the B.Sc.Eng. and M.Sc.Eng. degrees from the Faculty of Engineering, Mu'tah University, Al Karak, Jordan, in 2004 and 2007, respectively. He is currently pursuing the Ph.D. degree in electrical engineering with The University of Liverpool, U.K.

He was a Field Engineer in Amman, Jordan, from 2008 to 2009, and a Lecturer with the Department of Electrical Engineering, Mu'tah University, from 2009 to 2012. His current research interests include multiple-input and multiple-output and diversity antennas, dielectric resonator antennas and planar antennas, and microwave circuits.